Ultralong-Range Rydberg Bimolecules

Rosario González-Férez,[1,2,*] Janine Shertzer,[2,3] and H. R. Sadeghpour[2]
[1]Instituto Carlos I de Física Teórica y Computacional, and Departamento de Física Atómica, Molecular y Nuclear, Universidad de Granada, 18071 Granada, Spain
[2]ITAMP, Center for Astrophysics, Harvard & Smithsonian, Cambridge, Massachusetts 02138 USA
[3]Department of Physics, College of the Holy Cross, Worcester, Massachusetts 01610, USA

(Received 7 July 2020; accepted 5 January 2021; published 27 January 2021)

We predict that ultralong-range Rydberg bimolecules form in collisions between polar molecules in cold and ultracold settings. The interaction of Λ-doublet nitric oxide (NO) with long-lived Rydberg NO(nf, ng) molecules forms ultralong-range Rydberg bimolecules with GHz energies and kilo-Debye permanent electric dipole moments. The Hamiltonian includes both the anisotropic charge-molecular dipole interaction and the electron-NO scattering. The rotational constant for the Rydberg bimolecules is in the MHz range, allowing for microwave spectroscopy of rotational transitions in Rydberg bimolecules. Considerable orientation of NO dipole can be achieved. The Rydberg molecules described here hold promise for studies of a special class of long-range bimolecular interactions.

DOI: 10.1103/PhysRevLett.126.043401

Rydberg spectroscopy is one of the most precise techniques in the AMO physics toolkit to probe core interactions, perform cavity quantum electrodynamics [1], diagnose environmental influence in laboratory and astrophysical gases [2,3], engineer strong quantum correlations, and transmit quantum entanglement over macroscopic distances [4]. In cold and pristine ultracold AMO traps, Rydberg interactions with surrounding atoms or molecules may, under certain conditions, lead to the formation of special long-range Rydberg molecules [5,6]. Such Rydberg molecules have proven to be fertile ground for investigating novel few-body phenomena, many-body quantum correlations [7–9], and exotic ionic interactions [10,11]. To date, ultracold Rydberg excitations have been performed in a target atom—usually an alkali metal or alkaline earth atom [8,12].

Ultracold polar molecules have more accessible internal degrees of freedom than ultracold atoms, which can be engineered for simulations of chemical reactions [13–15], many-body interactions [16,17], and information processing in the quantum limit [18,19]. As with Rydberg systems, polar molecules can possess large dipole moments, making them amenable to control and manipulation. In addition, interactions involving molecules are fundamental to chemical synthesis, whose studies are in vogue in cold and ultracold traps as densities increase [20–23]. In most cold and ultracold settings, atom-molecule or molecule-molecule collisions often are exothermic, releasing energy leading to losses from the trap. Elaborate schemes to control and shield trapped molecules from such deleterious encounters are proposed [24–31].

Here, we investigate a particular class of bimolecular interactions, facilitated by Rydberg excitation in a Λ-doublet molecule (NO), leading to formation of exotic Rydberg bimolecules, whose electronic and rovibrational properties can be readily controlled. Because the Λ-doublet transitions can be precisely measured, such molecules are leading candidates for searches for the variation of fine-structure constant and electron to proton mass ratio [32].

Nitric oxide is a Λ-doublet molecule and has been extensively studied for its numerous applications across physics and chemistry. NO is an atmospheric constituent, which plays a large role in the chemistry and heat budget of the thermosphere, and at lower altitudes is a catalyst in depleting atmospheric ozone [33]. Because NO is also a neurotransmitter and neurotoxic [34,35], there is practical interest in NO detection. A recent promising technique for detection of NO concentration with high sensitivity is through Rydberg excitation in NO [36].

There are a number of unique features of Rydberg NO-NO bimolecular interactions at large distances, see Fig. 1: (a) hybridization of nearby Λ-doublet opposite parity states is efficient even when molecules possess permanent electric dipole moments (PEDM) much below the Fermi-Teller critical dipole, $d_{\mathrm{NO}} \sim 0.16$ D $< d_c \sim 1.63$ D [37–39], (b) long-lived high electronic angular momentum Rydberg bimolecular states (nf and ng) with small, but nonzero quantum defects, with extremely large PEDM (a few kilo-Debye) exist, rendering microwave transitions in such molecules possible, and (c) highly oriented NO dipoles form which can be coherently controlled for ultracold Rydberg chemistry, imaging of the molecular structure, and quantum information processing [40].

The Born-Oppenheimer (BO) Hamiltonian for the Rydberg NO-NO bimolecular interaction at large distances can be written as

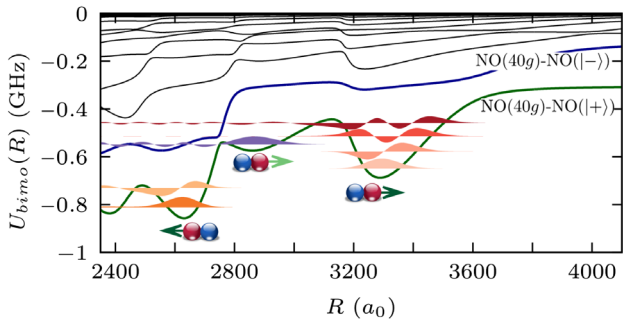

FIG. 1. $^3\Sigma^+$ Born-Oppenheimer potential energy curves near the NO($40g$)-NO($X^2\Pi_{1/2}$) thresholds. The molecular Λ-doublet splitting are identified by $|+\rangle$ and $|-\rangle$ labels. The wave functions of long-lived Rydberg bimolecular states are shown at the energy level. The magnitude and direction of orientation of the NO molecular dipole for each electronic well are also shown. All the interactions in the Hamiltonian (2) are included in obtaining these potential curves.

$$H = H_{\mathrm{Ryd}} + H_{\mathrm{NO}} + H_{e\text{-NO}}, \tag{1}$$

where H_{Ryd} is the Hamiltonian for the NO Rydberg molecule and $H_{\mathrm{NO}} = E_+|+\rangle\langle+| + E_-|-\rangle\langle-|$ is a two-state Λ-doublet Hamiltonian for NO, with a splitting $E_- - E_+ = 205.95$ MHz [39].

The Hamiltonian $H_{e\text{-NO}}$ contains the Rydberg electron and core interacting with the NO PEDM and the scattering of the Rydberg electron from NO,

$$H_{e\text{-NO}}(\mathbf{R},\mathbf{r}) = -\mathbf{d}_{\mathrm{NO}}\cdot\mathbf{F}_e(\mathbf{R},\mathbf{r}) + 2\pi a_S(k)\delta(\mathbf{r}-\mathbf{R}) + 6\pi a_P^3(k)\delta(\mathbf{r})\overleftarrow{\nabla}\cdot\vec{\nabla}, \tag{2}$$

where $\mathbf{r}$ and $\mathbf{R}$ are the positions of the Rydberg electron and NO($X^2\Pi_{1/2}$) with respect to the NO^+ core, respectively. The first term in Eq. (2) describes the interaction of the NO^+ core and the Rydberg electron with the NO($X^2\Pi_{1/2}$) PEDM $\mathbf{d}_{\mathrm{NO}}$. The internal field due to the Rydberg electron and core, $\mathbf{F}_e(\mathbf{R},\mathbf{r}) = e[(\mathbf{r}-\mathbf{R})/|\mathbf{r}-\mathbf{R}|^3 + \mathbf{R}/R^3]$, hybridizes the Λ-doublet states $|+\rangle$ and $|-\rangle$ of NO($X^2\Pi_{1/2}$). The total angular momentum excluding spin couples to $F_e(Z,z)$, while the other two perpendicular components of this electric field do not contribute to the interaction. Because there is no additional external electric field, the NO($X^2\Pi_{1/2}$) internuclear axis is taken to be along the Z axis.

The last two terms in Eq. (2) describe the Rydberg electron collision with NO. These two terms, respectively, reflect the contributions to the low-energy electron-molecule scattering in the $L=0$ (S-wave) and $L=1$ (P-wave) scattering partial waves [12,41,42]. The S-wave scattering length in the Fermi pseudopotential is, $a_S(k) = -\tan[\delta_S(k)]/k$, where $\delta_S(k)$ the $L=0$ scattering phase shift, and the scattering volume, $a_P^3(k) = -\tan[\delta_P(k)]/k^3$, where $\delta_P(k)$ the $L=1$ scattering phase shift, diverges at the position of an $L=1$ scattering resonance. Electron scattering from NO($X^2\Pi_{1/2}$) can form negative ions, $NO^-(X^3\Sigma^-)$. The electron affinity of NO has been measured by Alle *et al.* [43], $E_A = 33 \pm 10$ meV. In elastic electron scattering from NO$[X^2\Pi_{1/2}(\nu=0)]$, there exists a low-energy resonance at ∼100 meV. This resonance has been measured [44,45] in the channel $\{e^- + \mathrm{NO}[X^2\Pi_{1/2}(\nu=0)] \rightarrow \mathrm{NO}^-[X^3\Sigma(\nu'=1)]\}$; there are additional $\mathrm{NO}^-[X^3\Sigma(\nu'>1)]$ resonances, which appear in the inelastic channels. The fundamental vibrational frequency in NO($X^2\Pi_{1/2}$) is 236 meV [46].

Both NO and NO^+ have PEDM, and the resulting dipole-dipole interaction has also been incorporated in the Hamiltonian (1). For the NO(nl)-NO bimolecules, at separations of hundreds a_0, these dipolar interactions are several orders of magnitude smaller than the dominant charge-dipole interactions.

The Hamiltonian matrix is constructed from a basis set comprised of electronic Rydberg NO and molecular doublet orbitals, and the corresponding Schrödinger equation, $H\mathbf{C} = U_{\mathrm{bimo}}(R)\mathbf{C}$, is solved to obtain the bimolecular Rydberg BO potential energy curves $U_{\mathrm{bimo}}(R)$, and the electronic wave function $\mathbf{C}$.

To obtain the wave functions and energies for the Rydberg NO, a quantum defect description is appropriate. The Rydberg NO BO potential can be written as

$$U_{n\Lambda}(R_{\mathrm{NO}}) = U^+(R_{\mathrm{NO}}) - \frac{1}{2(n-\mu_\Lambda)^2}, \tag{3}$$

where $U^+(R_{\mathrm{NO}})$ is the ground-state BO potential curve for $NO^+(X^1\Sigma^+)$ and Λ is the projection of Rydberg electron orbital quantum number l on R_{NO}. The quantum defect μ_Λ depends on n and R_{NO}. In our analysis, R_{NO} is fixed at the equilibrium separation, $R_{\mathrm{NO}} = 2.175$ a_0. The quantum defects were calculated by Rabadán and Tennyson using a 12-state R-matrix method [47]. The Rydberg electron wave functions and energies for different molecular symmetries were obtained by solving the hydrogenic Schrödinger equation for noninteger values of n [48–50] using the finite element method. We note that frame transformation multichannel quantum defect theory [51] is a compact formulation of Rydberg electron interaction with molecular core electrons. In Rydberg NO, for instance, it results in mixing of Hund's cases (d) and (b) molecular symmetries. This mixing is particularly important at low orbital angular momenta, when the electron spends considerable time near the core and Rydberg energies will depend on the ion rotational quantum numbers [52]. Here, we are interested in formation of ultralong-range Rydberg bimolecules when the NO molecules are excited into high orbital angular momentum states, nf and ng.

Figure 2(a) presents the BO potential energy curves when *only* the charge-dipole interaction is included in the

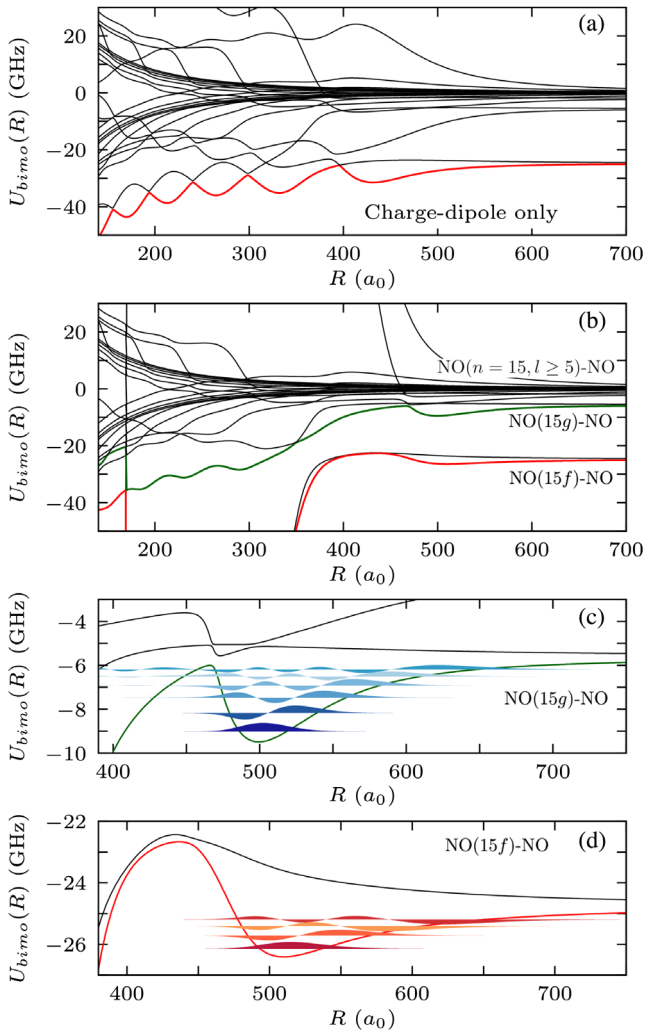

FIG. 2. BO potential energy curves of the NO($n = 15$, $l \geq 3$)-NO($X^2\Pi_{1/2}$) ultralong-range Rydberg bimolecule including (a) the charge-dipole only and (b) all the interactions in the Hamiltonian (2). Details of the curves including all interactions near the (c) NO(15g)-NO($X^2\Pi_{1/2}$) and (d) NO(15f)-NO($X^2\Pi_{1/2}$) dissociation thresholds; the vibrational wave functions are shown at the energy level. The bound states near the avoided crossing in (c) are quantum reflected states [55].

Hamiltonian (2) [53,54]. The near-degenerate Λ-doublet combined with the small quantum defects of the nf and ng Rydberg states give rise to several potential wells supporting bound vibrational levels. By taking into account the low energy scattering of the Rydberg electron with NO, the complexity of these electronic states is significantly enhanced in Fig. 2(b). Because of the interplay of charge-dipole interaction and $e^- - \mathrm{NO}$ collision, deep molecular binding occurs in the outerwell potentials at large distances ($R \sim 500$ a_0), which are pushed out due to the repulsive electron scattering length; see the NO(15f)-NO($X^2\Pi_{1/2}$) and NO(15g)-NO($X^2\Pi_{1/2}$) BO potential curves in Figs. 2(d) and 2(c), respectively. The outer wells support bound levels with 200–800 MHz vibrational spacing. At smaller distances, $R \lesssim 400$ a_0, the P-wave resonance introduces avoided crossing and l mixing among the potential energy curves, destroying several inner wells visible in Fig. 2(a).

Because of proximity to hydrogenic degenerate manifolds, the nf and ng Rydberg states have considerable l-mixed character, giving rise to long lifetimes. For the nf states, lifetimes of 10–50 ns have been measured [56], whereas ng states have lifetimes of $0.15\ \mu\mathrm{s} < \tau < 0.6\ \mu\mathrm{s}$ for $30g < nl < 55g$, against predissociation and vibrational autoionization [57]. Because of the l mixing, the NO(15f)-NO($X^2\Pi_{1/2}$) and NO(15g)-NO($X^2\Pi_{1/2}$) bimolecules possess fairly large PEDM, ∼0.5 kD [58], along their internuclear axis. The bimolecules in the potential wells in Figs. 2(c) and 2(d), maintain the NO dipole in full orientation away the NO^+ core; the orientation is computed as $\langle\psi|+\rangle\langle-|\psi\rangle$, with $|\psi\rangle$ being the total wave function. The rotational constant for the $n = 15$ Rydberg NO bimolecules is about 0.5 MHz. As a consequence, microwave spectroscopy of rotational transitions now becomes feasible, and realistic microwave Rabi frequencies of 1–10 MHz can be achieved.

The BO potential energy curves converging to the NO($40, l \geq 3$)-NO($X^2\Pi_{1/2}$) dissociation threshold, are shown in Fig. 3. Because the P-wave resonance affects the energies at shorter distances, its effect on the NO(40f) and NO(40g) Rydberg bimolecular states is reduced. The potential curves converging to NO(40f) in Figs. 3(b) and 3(c) support deep vibrational levels. The PEDMs for NO(40f)-NO($X^2\Pi_{1/2}$) and NO(40g)-NO($X^2\Pi_{1/2}$) electronic states are in the 5–7 kD range. The Λ-doublet separated upper curve in NO(40f), for instance, in Fig. 3(b) has a double well with well-separated molecular states. The right and left wells correspond to NO molecular orientation away and toward the Rydberg molecular core [53]. The degree of NO dipole orientation is roughly 40%. This orientation is even larger for the NO(40g)-NO($X^2\Pi_{1/2}$) bimolecules in Fig. 1, reaching 99% in the inner and outer wells and 60% in the central well.

The Rydberg bimolecules can be experimentally created by excitation of the main optical transition in NO, $A^2\Sigma^+(\nu' = 0, N' = 0) \leftarrow X^2\Pi(\nu = 0, N = 0)$ at 225 nm in the γ band [36,52,59]. The $A^2\Sigma^+$ state has configuration interaction coefficients, 94% ($l = 0$), 1% ($l = 1$), and 5% ($l = 2$) [60], allowing for excitation of np ($\Delta N = 0$), np and nf ($\Delta N = 0, \pm 2$) optical transitions. Additional transitions, to $H'(^2\Pi)$ or $H(^2\Sigma^+)$ electronic states, and Rydberg $^2\Sigma^+$ states [61] can produce NO(nf)-NO and NO(ng)-NO Rydberg bimolecules. In addition, NO(nf, ng)-NO Rydberg bimolecules can be formed by excitation near the $X^1\Sigma^+$ electronic ground state of NO^+ ion with a 328 nm pulsed laser [36,57]. In Ref. [57], the NO(4f) state is an intermediary state to NO(ng) Rydberg levels.

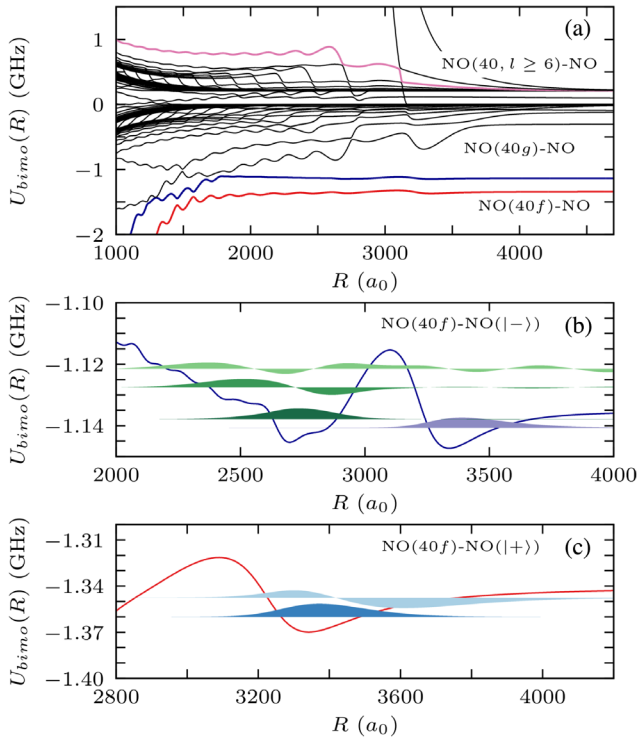

FIG. 3. (a) BO potential energy curves of the NO($n = 40, l \geq 3$)-NO($X^2\Pi_{1/2}$) Rydberg bimolecule including all the interactions in the Hamiltonian (2). Details of the curves near the (b) NO($40f$)-NO($X^2\Pi_{1/2}, |-\rangle$) and (c) NO($40f$)-NO($X^2\Pi_{1/2}, |+\rangle$) dissociation thresholds; the vibrational wave functions are shown at the energy level. For illustration, we highlight the magenta curve in (a), which is completely blueshifted and supports a number of bound vibrational levels in the different wells. In (b), the degree of orientation of the NO dipole in the two outer wells is, respectively, 0.33 and −0.40, i. e., the NO dipole is pointing away from the NO^+ core and toward the core, respectively. Whereas in (c), the degree of orientation in the two bound states is, respectively, 0.43 and 0.32.

In summary, we describe the formation of a new class of ultralong-range molecules, comprised of the interaction of a Rydberg molecule (here NO) with another ground state Λ-doublet (NO) molecule. Long-lived Rydberg bimolecular states with enormous PEDM are predicted. Because the rotational constant of such Rydberg bimolecules are in the 0.1–1 MHz range, microwave spectroscopy of rotational transitions are now within the realm of possibility with realistic microwave Rabi frequencies. Cold and ultracold NO samples could be made in a supersonic beam [59,62,63] and held in an electrostatic trap [63], and via Sisyphus cooling techniques [64], respectively. In a thermal molecular gas, rotational states are Boltzmann distributed, but yet it is possible for the main rotational transition to be observed. Because the Rydberg electron couples to the spin symmetries in the molecule, the interaction terms in Eq. (2) can be spin mixed and BO potentials with mixed spin and orbital angular momenta emerge, which can be manipulated and controlled with small magnetic fields. With a proliferation of activities in trapping of doublet molecules, in particular in optical tweezers [65] and magnetic traps [66], Rydberg excitation in such molecules in cold and ultracold settings is within reach. The ultralong-range Rydberg bimolecules predicted in this work hence open a new vista into cold bimolecular collisions and control interactions.

R. G. F. acknowledges financial support of the Subprograma Estatal de Movilidad of the Programa Estatal de Promoción del Talento y su Empleabilidad en I+D+i (MECD), the Spanish Project FIS2017-89349-P (MINECO), and the Andalusian research group FQM-207. R. G. F. did this work as a Fulbright fellow at ITAMP at Harvard University. We wish to thank Seth Rittenhouse and Frederic Hummel for helpful suggestions. H. R. S. acknowledges a visit to University of Stuttgart as part of the GiRyd program, where the initial discussions were carried out.

*rogonzal@ugr.es

[1] S. Haroche, Rev. Mod. Phys. **85**, 1083 (2013).
[2] N. Allard and J. Kielkopf, Rev. Mod. Phys. **54**, 1103 (1982).
[3] J. Szudy and W. Baylis, Phys. Rep. **266**, 127 (1996).
[4] M. Saffman, T. G. Walker, and K. Mølmer, Rev. Mod. Phys. **82**, 2313 (2010).
[5] C. H. Greene, A. S. Dickinson, and H. R. Sadeghpour, Phys. Rev. Lett. **85**, 2458 (2000).
[6] V. Bendkowsky, B. Butscher, J. Nipper, J. P. Shaffer, R. Löw, and T. Pfau, Nature (London) **458**, 1005 (2009).
[7] R. Schmidt, H. R. Sadeghpour, and E. Demler, Phys. Rev. Lett. **116**, 105302 (2016).
[8] F. Camargo, R. Schmidt, J. D. Whalen, R. Ding, G. Woehl, S. Yoshida, J. Burgdörfer, F. B. Dunning, H. R. Sadeghpour, E. Demler, and T. C. Killian, Phys. Rev. Lett. **120**, 083401 (2018).
[9] J. Sous, H. R. Sadeghpour, T. C. Killian, E. Demler, and R. Schmidt, Phys. Rev. Research **2**, 023021 (2020).
[10] F. Engel, T. Dieterle, T. Schmid, C. Tomschitz, C. Veit, N. Zuber, R. Löw, T. Pfau, and F. Meinert, Phys. Rev. Lett. **121**, 193401 (2018).
[11] F. Hummel, P. Schmelcher, H. Ott, and H. R. Sadeghpour, New J. Phys. **22**, 063060 (2020).
[12] J. P. Shaffer, S. T. Rittenhouse, and H. R. Sadeghpour, Nat. Commun. **9**, 1965 (2018).
[13] J. M. Doyle, B. Friedrich, and E. Narevicius, Chem. Phys. Chem. **17**, 3581 (2016).
[14] L. Carr, D. DeMille, R. Krems, and J. Ye, New J. Phys. **17** (2015), and references therein, **11**, 055049 (2009) and references therein.
[15] G. Quéméner and P. S. Julienne, Chem. Rev. **112**, 4949 (2012).
[16] H. P. Büchler, A. Micheli, and P. Zoller, Nat. Phys. **3**, 726 (2007).
[17] L. De Marco, G. Valtolina, K. Matsuda, W. G. Tobias, J. P. Covey, and J. Ye, Science **363**, 853 (2019).
[18] S. F. Yelin, K. Kirby, and R. Côté, Phys. Rev. A **74**, 050301(R) (2006).

[19] A. André, D. DeMille, J. M. Doyle, M. D. Lukin, S. E. Maxwell, P. Rabl, R. J. Schoelkopf, and P. Zoller, Nat. Phys. **2**, 636 (2006).

[20] S. Ospelkaus, K.-K. Ni, D. Wang, M. H. G. de Miranda, B. Neyenhuis, G. Quéméner, P. S. Julienne, J. L. Bohn, D. S. Jin, and J. Ye, Science **327**, 853 (2010).

[21] M.-G. Hu, Y. Liu, D. D. Grimes, Y.-W. Lin, A. H. Gheorghe, R. Vexiau, N. Bouloufa-Maafa, O. Dulieu, T. Rosenband, and K.-K. Ni, Science **366**, 1111 (2019).

[22] Y. Segev, M. Pitzer, M. Karpov, N. Akerman, J. Narevicius, and E. Narevicius, Nature (London) **572**, 189 (2019).

[23] P. D. Gregory, J. A. Blackmore, S. L. Bromley, and S. L. Cornish, Phys. Rev. Lett. **124**, 163402 (2020).

[24] A. V. Gorshkov, P. Rabl, G. Pupillo, A. Micheli, P. Zoller, M. D. Lukin, and H. P. Büchler, Phys. Rev. Lett. **101**, 073201 (2008).

[25] A. Crubellier, R. González-Férez, C. P. Koch, and E. Luc-Koenig, Phys. Rev. A **95**, 023405 (2017).

[26] T. Karman and J. M. Hutson, Phys. Rev. Lett. **121**, 163401 (2018).

[27] L. Lassablière and G. Quéméner, Phys. Rev. Lett. **121**, 163402 (2018).

[28] A. Christianen, M. W. Zwierlein, G. C. Groenenboom, and T. Karman, Phys. Rev. Lett. **123**, 123402 (2019).

[29] A. Crubellier, R. González-Férez, C. P. Koch, and E. Luc-Koenig, Phys. Rev. A **99**, 032710 (2019).

[30] T. Karman, Phys. Rev. A **101**, 042702 (2020).

[31] T. Xie, M. Lepers, R. Vexiau, A. Orban, O. Dulieu, and N. Bouloufa-Maafa, Phys. Rev. Lett. **125**, 153202 (2020).

[32] M. G. Kozlov, Phys. Rev. A **80**, 022118 (2009).

[33] L. Campbell and M. J. Brunger, Plasma Sources Sci. Technol. **22**, 013002 (2012).

[34] D. D. Thomas, L. A. Ridnour, J. S. Isenberg, W. Flores-Santana, C. H. Switzer, S. Donzelli, P. Hussain, C. Vecoli, N. Paolocci, S. Ambs, C. A. Colton, C. C. Harris, D. D. Roberts, and D. A. Wink, Free radical biology and medicine **45**, 18 (2008).

[35] S. A. Korneev, V. Straub, I. Kemenes, E. I. Korneeva, S. R. Ott, P. R. Benjamin, and M. O'Shea, J. Neurosci. **25**, 1188 (2005).

[36] J. Schmidt, M. Fiedler, R. Albrecht, D. Djekic, P. Schalberger, H. Baur, R. Löw, N. Fruehauf, T. Pfau, J. Anders, E. R. Grant, and H. Kübler, Appl. Phys. Lett. **113**, 011113 (2018).

[37] E. Fermi and E. Teller, Phys. Rev. **72**, 399 (1947).

[38] A. Gijsbertsen, W. Siu, M. F. Kling, P. Johnsson, P. Jansen, S. Stolte, and M. J. J. Vrakking, Phys. Rev. Lett. **99**, 213003 (2007).

[39] R. M. Neumann, Astrophys. J. **161**, 779 (1970).

[40] E. Kuznetsova, S. T. Rittenhouse, H. R. Sadeghpour, and S. F. Yelin, Phys. Rev. A **94**, 032325 (2016).

[41] A. Omont, J. Phys. **38**, 1343 (1977).

[42] H. R. Sadeghpour, J. L. Bohn, M. J. Cavagnero, B. D. Esry, I. I. Fabrikant, J. H. Macek, and A. R. P. Rau, J. Phys. B **33**, R93 (2000).

[43] D. T. Alle, M. J. Brennan, and S. J. Buckman, J. Phys. B **29**, L277 (1996).

[44] A. Zecca, I. Lazzizzera, M. Krauss, and C. E. Kuyatt, J. Chem. Phys. **61**, 4560 (1974).

[45] M. Tronc, A. Huetz, M. Landau, F. Pichou, and J. Reinhardt, J. Phys. B **8**, 1160 (1975).

[46] M. Olman, M. McNelis, and C. Hause, J. Mol. Spectrosc. **14**, 62 (1964).

[47] I. Rabadán and J. Tennyson, J. Phys. B **30**, 1975 (1997).

[48] D. Bates and A. Damgaard, Philos. Trans. R. Soc. London **242**, 101 (1949).

[49] L. Infeld and T. E. Hull, Rev. Mod. Phys. **23**, 21 (1951).

[50] V. A. Kostelecký and M. M. Nieto, Phys. Rev. A **32**, 3243 (1985).

[51] C. H. Greene and C. Jungen, in *Advances in Atomic and Molecular Physics*, Vol. 21 (Academic Press, New York, 1985), pp. 51–121.

[52] M. J. J. Vrakking, J. Chem. Phys. **105**, 7336 (1996).

[53] S. T. Rittenhouse and H. R. Sadeghpour, Phys. Rev. Lett. **104**, 243002 (2010).

[54] R. González-Férez, H. R. Sadeghpour, and P. Schmelcher, New J. Phys. **17**, 013021 (2015).

[55] V. Bendkowsky, B. Butscher, J. Nipper, J. B. Balewski, J. P. Shaffer, R. Löw, T. Pfau, W. Li, J. Stanojevic, T. Pohl, and J. M. Rost, Phys. Rev. Lett. **105**, 163201 (2010).

[56] M. J. J. Vrakking and Y. T. Lee, Phys. Rev. A **51**, R894 (1995).

[57] A. Fujii and N. Morita, J. Chem. Phys. **103**, 6029 (1995).

[58] D. Booth, S. T. Rittenhouse, J. Yang, H. R. Sadeghpour, and J. P. Shaffer, Science **348**, 99 (2015).

[59] J. P. Morrison, C. J. Rennick, J. S. Keller, and E. R. Grant, Phys. Rev. Lett. **101**, 205005 (2008).

[60] K. Kaufmann, C. Nager, and M. Jungen, Chem. Phys. **95**, 385 (1985).

[61] F. Munkes, Master's Thesis, University of Stuttgart, 2019.

[62] A. Deller and S. D. Hogan, J. Chem. Phys. **152**, 144305 (2020).

[63] A. Deller, M. H. Rayment, and S. D. Hogan, Phys. Rev. Lett. **125**, 073201 (2020).

[64] M. Zeppenfeld, B. G. U. Englert, R. Glöckner, A. Prehn, M. Mielenz, C. Sommer, L. D. van Buuren, M. Motsch, and G. Rempe, Nature (London) **491**, 570 (2012).

[65] L. Anderegg, L. W. Cheuk, Y. Bao, S. Burchesky, W. Ketterle, K.-K. Ni, and J. M. Doyle, Science **365**, 1156 (2019).

[66] B. C. Sawyer, B. L. Lev, E. R. Hudson, B. K. Stuhl, M. Lara, J. L. Bohn, and J. Ye, Phys. Rev. Lett. **98**, 253002 (2007).